Arabian Journal of Chemistry (2022) **15**, 104127

King Saud University

Arabian Journal of Chemistry

www.ksu.edu.sa
www.sciencedirect.com

ORIGINAL ARTICLE

Characterization of lignin and lignin-derivatives from biomass. Application as expander of Lead-acid battery

Maryame Tghos Naim [a], Marta Lara-Serrano [c], Alberto F. Romero [a,b], Silvia Morales-delaRosa [c], Jose M. Campos-Martín [c], Juan Ramón Avilés Moreno [a,*], Pilar Ocón [a]

[a] *Universidad Autónoma de Madrid (UAM), Departamento de Química Física Aplicada, C/Francisco Tomás y Valiente 7, 28049 Madrid, Spain*
[b] *Exide Technologies, R&D Centre, 19200, Azuqueca de Henares, Spain*
[c] *Instituto de Catálisis y Petroleoquímica, CSIC, Grupo de Energía y Química Sostenible (EQS), C/Marie Curie, 2 Cantoblanco, 28049 Madrid, Spain*

Received 27 April 2022; accepted 12 July 2022
Available online 20 July 2022

KEYWORDS

Lignin;
Lignosulfonate;
Additives;
Lead acid batteries;
Physicochemical characterization

Abstract Expanders, as lignosulfonates, are crucial for a good performance of Pb/acid batteries. In the process of discharge, the Pb and the PbO_2 go to $PbSO_4$. The formed $PbSO_4$ is adsorbed on the surface of the Pb electrode and dramatically reduces the lifetime of the battery by the formation of big $PbSO_4$ crystals. In order to prevent that, the addition of expanders in the negative electrode is an economic solution to prevent the formation of big crystals. In this investigation, we propose the synthesis of several lignosulfonates obtained from lignin of many biomass origins. We have derivatized nine samples of lignin via microwave-assisted sulfonation, then we have characterized how efficient is the chosen synthesis method. The lignosulfonates obtained have been characterized by infrared spectroscopy (IR), proton nuclear magnetic resonance (^{1}HNMR), two-dimensional correlated spectroscopy (COSY), and elemental analysis to acquire some relevant information about their structure in terms of functional groups. In this way, three commercial lignosulfonates, Vanisperse A, Indulin AT, and Oakwood, have been selected as references for our comparisons. Moreover, we have checked their electrochemical properties, using electrochemical techniques to compare their behavior with respect to the commercial lignosulfonates. Finally, we have selected one of them and we have tested its performance as an expander in a Pb/acid battery.

* Corresponding author.
E-mail address: juan.aviles@uam.es (J. Ramón Avilés Moreno).
Peer review under responsibility of King Saud University.

Production and hosting by Elsevier

https://doi.org/10.1016/j.arabjc.2022.104127

That result is a very promising first approach, and we can conclude that lignosulfonates derivatives are a good and low-cost choice to improve the lifetime of Pb/acid batteries. In particular, it is shown that the incorporation of LignosB improves the cell formation as well as the first capacity (36.30% more) and the charge acceptance (63.16% more), being these relevant parameters in the performance of Pb/acid batteries.

1. Introduction

Cellulose, hemicelluloses, and lignin are the main components of the plant cell wall, linked together by a highly ordered matrix called lignocellulose (Rubin, 2008; Lara-Serrano et al., 2019). And for this reason, biopolymers are the most abundant on Earth (Pickett, 2018). Cellulose and hemicellulose are polymers based on carbohydrates, while lignin is a polymer made by cross-linking phenolic precursors. Lignin and hemicellulose, unlike cellulose, have different chemical compositions depending on the lignocellulose source treated. Because lignin is a complex heterogeneous branched polymer that, being linked and hemicellulose in the so-called "lignin-carbohydrate complexes" (Rubin, 2008; Lara-Serrano et al., 2019), it is necessary to carry out a fragmentation pretreatment to obtain it.

The annual production of lignin is 1.8 million tons, and they are used as pesticides, surfactants, stabilizers of colloidal suspensions, etc. (Aro and Pedram, 2017; Baumberger et al., 1997) Some of the most important characteristics of lignin are the following: contain most of the methoxy groups in wood, are resistant to acid hydrolysis, and easily oxidize. Also, they are soluble in hot bisulfite or alkalis, and they condense with phenols and thiols. If they are treated with nitrobenzene, in a hot alkaline medium, vanillin, syringaldehyde, or p-hydroxybenzaldehyde are obtained depending on their origin (Yang et al., 2017). Lignins are built of phenylpropanoid units, the most general being p-coumaryl alcohol, coniferyl alcohol, and sinapyl alcohol (Fig. 1). They are formed in the cytoplasm of plants through the "Shikimate pathway" (Chávez Sifontes and Domine, 2013) and are interconnected by C-C and C-O bonds (Dutta et al., 2018).

The proportion of the phenylpropanoid units in lignins depends on the type of plant from which it was extracted. It should be noted that in softwoods (conifers, gymnosperms) the percentage of p-coumaryl alcohol is less than 5% and that of coniferyl alcohol is more than 95%. In hardwoods (eucotyledons, angiosperms) p-coumaryl alcohol is between 0 and 8%, coniferyl alcohol between 25 and 50%, and sinapyl alcohol 45–75%. In herbs (monocotyledons, angiosperms), p-coumaryl alcohol is between 3 and 35%, coniferyl alcohol between 35 and 80%, and sinapyl alcohol between 20 and 55% (Chávez Sifontes and Domine, 2013). It is present in all vascular plants and is formed during the photosynthesis reaction (Chávez Sifontes and Domine, 2013).

It must be considered that lignins do not have structures that can be defined exactly and precisely, apart from the phenylpropanoid units mentioned above lignins also present modifications of those units. These units are obtained through oxidation reactions, which occur in plant cell walls, and which are catalyzed by peroxidase enzymes (Chávez Sifontes and Domine, 2013). Thus, the order of repetition of said units (main or derived) is not regular and their grouping will depend on the extraction method used and the type of plant (Yang et al., 2017). In addition, it should be noted that both lignins and lignosulfonates are recently being used in multiple applications, in addition to their well-known action as expanders in lead batteries, ranging from the application as biosensors, enzymatic action in biomass degradation processes or, even obtaining lignin-based nanoparticles (Wang et al., 2022; Wang et al., 2021; Lou et al., 2014; Guo et al., 2021; Tang et al., 2020; Tian et al., 2019; Gu et al., 2019; Yao et al., 2017; Vermaas et al., 2015; Crestini et al., 2011; Liu et al., 2022).

There are numerous pretreatments for the fragmentation of lignocellulosic biomass described in the literature, however, some of the most innovative are among the chemical methods (Behera et al., 2014), which are capable of dissolving lignocellulosic biomass in a specific way, being able to separate cellulose, hemicellulose, and lignin into enriched fractions. Some of these pretreatments use ionic liquids (Lara-Serrano et al., 2019; Lavarda et al., 2019), inorganic salts (Lara-Serrano et al., 2020; A:A. Awosusi, A. Ayeni, R. Adeleke, M.O. Daramola, 2017), or by using organic solvents that are more environmentally friendly such as those used in the OrganoCat method (Grande et al., 2015; Stiefel et al., 2017; Weidener et al., 2021).

Lignosulfonates are derivative composites of lignin, they exhibit functional groups with a hydrophilic character such as methoxyl groups such as aldehydes, ketones, sulfonates, and carboxylic acids, on a hydrophobic backbone, mostly aromatic groups. This characteristic gives them a surface property as surfactants (Baumberger et al., 1997; Pérez Macías, 2017).

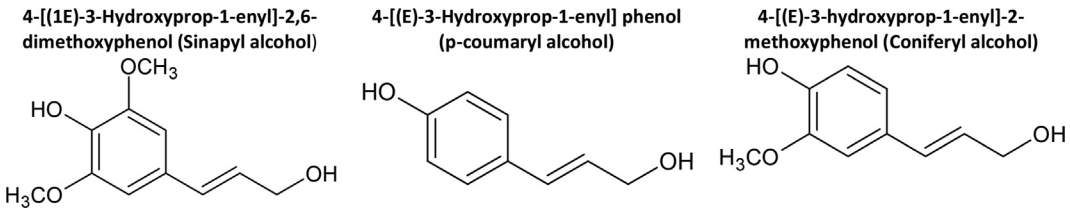

Fig. 1 Most common phenylpropanoid units of lignins.

The organic substances addition, type lignosulfonates, on the Pb-acid battery negative plate manufacturing has a positive effect on its performance. This effect has been known for a long time, and the mechanism of action has been studied by Pavlov (Pavlov et al., 1984; Pavlov et al., 2010; Zhang et al., 2022). These additives are called expanders together with black carbon and $BaSO_4$ (Myrvold, 2003). The lignosulfonates exert a very prominent effect on the specific surface and on the morphology of the negative active material (NAM), creating a skeleton on which the $PbSO_4$ crystals formed in the NAM can be deposited (Pavlov et al., 2000). Those act as anti-flocculating agents, preventing the agglutination of the $PbSO_4$ crystals and reducing their size (Yang et al., 2017). As an effect, the addition of lignosulfonates in the Pb/acid batteries, delays the charge/discharge reactions, but increases the capacity of the negative plates.

Not all lignosulfonates have the same functional groups, or the same molecular weights, it depends on a great extent on the starting lignins from which they have been obtained. Thus, lignins are one of the most abundant biopolymers in plants, along with cellulose and hemicellulose, and the greatest natural resource for obtaining aromatic compounds. Currently only 1–2% of the 50–70 millions of tons of lignin produced annually is used, evidencing its little application (Aro and Pedram, 2017).

The lignosulfonate molecular weight is of great importance, since the part with the highest molecular weight of the structure has a greater affinity for adhering to the surface of the lead electrode. However, the low molecular weight fragment forms complexes with the Pb^{+2} ions, leaving these in solution (Myrvold, 2003). Another factor that greatly influences the adsorption process is the pH: At low pH, a greater amount of lignosulfonate in solution is observed, indicating low adhesion to the surface of the negative electrode. Probably there is less interaction between the Pb^{+2} ions and lignosulfonates molecules due to the protonation of the phenolic, hydroxyl and carboxylic acid groups, and/or the partial protonation of the sulfonate groups (Myrvold, 2003).

In the battery discharge process the negative electrode is described as the oxidation of Pb to $PbSO_4$ compound, while in the positive electrode the reduction of PbO_2 to $PbSO_4$ also occurs. The charging process is the reverse of reactions (1) and (2) and the global reaction of these batteries is the one represented by equation (3).

Cathode (Positive electrode) :

$$PbO_2(s) + [HSO_4]^-(aq) + 3H^+(aq) + 2e^- \leftrightarrow PbSO_4(s) + 2H_2O(l). \quad (1)$$

Anode (Negative electrode) :

$$Pb(s) + [HSO_4]^-(aq) \leftrightarrow PbSO_4(s) + H^+(aq) + 2e^-. \quad (2)$$

Global reaction :

$$Pb(s) + PbO_2(s) + 2H_2SO_4(l) \leftrightarrow 2PbSO_4(s) + 2H_2O(l) \quad (3)$$

The nominal voltage of the Pb/acid battery is 2 V. It must be considered that, in the charging process, secondary reactions occur (Ruetschi, 1977). Thus, the electrolysis of water at the end of the battery charge occurs and therefore the evolution of hydrogen and oxygen. Nevertheless, water consumption can be minimized by recombination mechanisms. Adequate compression of the plates and the use of porous spacers Absorbed Glass Mat (AGM) allows the recombination between oxygen and hydrogen (Ruetschi, 1977). The sulphation of the negative plate is an important failure mode in these batteries, and it occurs as a priority when it works in a Partial State of Charge (PSoC) operating mode as required in hybrid vehicles. The formation of irreversible $PbSO_4$ crystals, which directly interferes to the electrochemical reaction (Rand et al., 2004) could be partially avoid with the addition of expanders.

The Pb/acid battery is one of the most widely used energy storage systems since the late nineteenth century. This system has been able to respond to numerous demands of society, and for now irreplaceable, application as an autonomous source of energy in transport vehicles, or as a power supply system in telecommunications or remote areas. More recently they are being used in the development of hybrid and/or electric vehicles (Pérez Macías, 2017; Zhang et al., 2021).

Our work is focused on the characterization of Lignins from pruning and cane biomass and their corresponding lignosulfonates derivatives. We present a microwave-assisted synthesis method which was successful for the obtention of lignosulfonates but with a variable proportion of functional groups. We studied the effect of lignosulfonate addition effect on the oxidation / reduction process of the Pb electrode in acid media finding similar behavior to the commercial lignosulfonates Vanisperse A, Indulin AT and Oak Wood. Moreover, their adsorption on the working electrode causes an increase in both anodic and cathodic process, indicating their effectiveness in controlling the formation of $PbSO_4$ crystals. Finally, our derivatives included in Pb/acid battery improve the cell formation as well as the first capacity (C_{20}) and the charge acceptance in comparison with Vanisperse A being these characteristics very important for the performance of the battery. Our characterization reveals a valuable conclusion for the achievement of priceless derivatives for their application as expanders in Pb/acid batteries.

2. Material and methods

2.1. Synthesis of lignosulfonates: MW

All the lignins used in this work are attained from pruning and bagasse cane biomass (see Scheme 1). The extraction process is described in SI (Schemes A1, A2 and A3). In short, those processes involve aqueous-organic extraction techniques following by vacuum filtration and washing of the extracted solid. To obtain lignins LigA1 and LigA1′, the process is described in

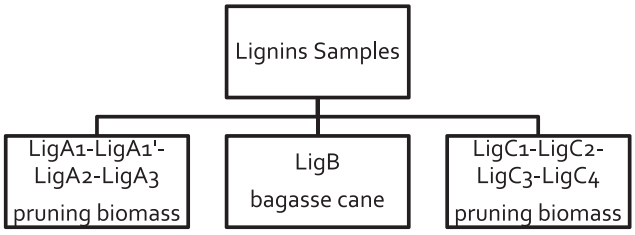

Scheme 1 Origin of Lignin samples characterized in this work.

Scheme A1 (Lara-Serrano et al., 2019). In the case of the lignins LigA2 and LigA3, the process is described in Scheme A2 (Ysambertt, 2009), and the obtaining of the lignins LigB, LigC1, LigC2, LigC3 and LigC4 are set forth in Scheme A3.

The synthesis process chosen to achieve the lignosulfonates consists in microwave-assisted sulfonation, a process proposed by F. Ysambertt, et al. (Ysambertt, 2009) The sulfonation process can be summarized in a six-steps synthesis: i) First, we mix lignin with a Na_2SO_3 (22 % m/v) and Na_2CO_3 (4 % m/v) solutions in a PVC reactor; ii) Second, we apply 10 microwave irradiation cycles of 6 s at 550 W (10 s off between cycles) getting a solution with suspended particles; iii) Third, we add between 6 and 10 drops of concentrated H_2SO_4 and 10% of $NaHCO_3$ to get a neutral-basic pH; iv) We centrifugate until supernantant can be separated and stored; v) We add concentrated H_2SO_4 until precipitation of lignosulfonate; vi) Finally, we separate by centrifugation and we dry at 50 °C. See Scheme A4 for more information. Additionally, Table A1 shows some experimental details about the solutions preparation process and their respective concentration, in addition to the used volumes in the synthesis process. All syntheses were done in duplicate. See Table A1 for more information about the synthesis process.

Commercial lignosulfonates, Vanisperse A, Indulin AT and Oak Wood (Borregaard Ligno Tech) were studied to compare the results.

2.2. Physico-chemical characterization

2.2.1. FT-IR with ATR module

Fourier-transform spectrophotometer (FT-IR, PerkinElmer Spectrum Two) coupled to an ATR (Attenuated Total Reflectance, Perkin Elmer) was used to identify the main functional groups of the lignins and lignosulfonates samples. For each IR measurement, the experimental conditions were 32 scans, 2 cm^{-1} of resolution, and 4000 – 450 cm^{-1} spectral range. The spectra were normalized to the main absorption band and baseline corrected.

2.2.2. NMR and COSY

All the ^{1}HNMR and COSY (^{1}H–^{1}H) spectra were measured using a low-medium field Bruker Avance III-HD Nanobay 300 MHZ. We work with a resonance frequency of 300 MHz, being the ^{1}H atom of study.

Firstly, the ^{1}HNMR spectra bands are analyzed in order to determine their chemical shift of the different hydrogens present in the samples. And secondly, the COSY (^{1}H–^{1}H) spectra determines the correlation between these H groups. The signals reflect two-bond and three-bond couplings.

2.2.3. Elemental analysis

The objective of elemental analysis is to determine the amount of carbon, hydrogen, nitrogen, and sulfur by oxidizing the sample, through a total combustion process, in an atmosphere of pure oxygen. The products obtained are CO_2, H_2O, N_2 and SO_2. A carrier gas (He) drags these products to selective sensors that are responsible for quantifying CO_2, H_2O and SO_2. N_2 is quantified by differential heat conductivity. The LECO CHNS-932 analyzer is used in this work, being the minimum quantifiable content of the elements around 0.2%. From elemental analysis, sulfonation degree can be estimated, which could be defined as the millimolar content of sulfonic acid per gram of lignosulfonates, is an important structure parameter which is related to many physicochemical properties of lignosulfonates such as water solubility, dispersing performance, surface activity, and complexation ability (Li et al., 2019).

2.2.4. Electrochemical characterization

The electrochemical test was performed in a three-electrodes cell, using Pb as a working electrode, Pb as counter electrode and Ag/AgCl, KCl (s) as reference electrode. Solutions with lignosulfonate were around 45 ppm in H_2SO_4 acid 1.28 g cm^{-3}. The lignosulfonate is incorporated into a beaker containing the minimum amount of sulfuric acid and it is sonicated to facilitate the homogeneity in the solution. In general variation between (54 and 46 ppm) was obtained.

Cyclic voltammetry (CV) from −1 V to 0,0 V at scan rate of 5 mV s^{-1} was carried out. The set-up consists in 5 scans in a blank solution (H_2SO_4) and then the lignosulfonate solution was added and 17 cycles at 5 mV s^{-1} was carried out.

Pb/acid battery, Cell assembly: The study was carried out by 2 V/ 0.230 Ah cells which were prepared through 2 positive and 1 negative plates (2:1 system) and were compressed between two methacrylate sheets and partially submerged in 1.28 g cm^{-3} H_2SO_4 (100 mL). The lignosulfonate selected as an expander was LignosB (0,3% vs PbO) and for the Control Lig Cells Vanisperse A (0,3% vs PbO) is incorporated because represents the state of the art in the field of Pb/acid batteries. No carbon additive has been added to appreciate more clearly the effect of the lignosulfonates.

Cell parameters: I_{20} = 0.0115 A; C_{20} = 0.230 Ah; Geometrical area / face = 2.52 cm2; NAM = 1.85 g; PAM = 1.85 g.

The electrical testing was performed at 25.0 °C and it consisted in two capacity tests (C_{20}), an charge acceptance (CA) test, and a pseudo-Tafel test. The formation profile at 40 °C selected for 2 V/ 0.230 Ah.

To check the low discharge rate performance Capacity (C_{20}) was carried out. After the cell formation and no more of seven days, the battery was discharged at 0.0115 A (I_{20}) with a 1.75 V voltage cut-off. Then, the cell was recharged during 24 h with a Constant Current Constant Voltage (CCCV) at 2.67 V and 0.0575 A (5 × I_{20}).

Charge acceptance (CA): After a resting period of 48–72 h at 25 ± 2 °C, the battery was charged through constant current constant voltage (CCCV) at 2.67 V and 0.0575 A (5 × I_{20}). After, the battery was resting 1 h and it was discharged at 0.0115 A (I_{20}) for 2 h until to get the 90% SoC. Then, it was stored at 25 ± 2 °C for 72 h (sulfation period). Later, the charge run at 2.4 ± 0.1 V with the highest current limit (Imax = 5 or 10 A) for 60 s. During the charge, the current was measured and recovered every 0.1 s. Ultimately, the battery was recharged during 24 h running through a CCCV at 2.67 V and 0.0575 A (5 × I_{20}).

Tafel-polarization curves: After the CA test and resting for 48–72 h at 25 ± 2 °C, a set of currents passed through the charged battery, so, the battery was charged with progressive current values at different time periods: 46 mA / 50 min; 23 mA / 20 min; 9.2 mA / 20 min; 4.6 mA / 20 min; 2.3 mA / 20 min; 0.92 mA / 15 min; 0.46 mA / 10 min and 0.23 mA / 10 min.

3. Results and discussion

3.1. Synthesis

Prior to the lignosulfonates synthesis, the characterization of lignins has been carried out to consider the main properties in order to successfully approach the corresponding derivatization.

Initially, the two lignin samples LigA1 and LigA1′ are characterized by IR. In both samples (Fig. 2) a broad band of maximum absorption is observed at approximately 3300 cm^{-1}, possibly due to O-H and N-H stretching vibrations, involved in hydrogen bonds networks. The band around 3150 cm^{-1} is assigned to aromatic C-H stretching. The weak bands around 3000 cm^{-1} indicate the presence of sp3 CH stretching, at 2930 cm^{-1} and a shoulder at 2850 cm^{-1} (possible carbonyl CHO stretching) but we do not see any clear band in the C = O stretching. This evidence could be since the proportion of carbonyl monomers is small (Reyes et al., 2015). The signals at 1600 cm^{-1} are assigned to C = C stretching. Lastly, two bands due to C-O stretching stand out, the first appears at approximately 1150 cm^{-1} referred to phenols while the second appears at 1030 cm^{-1} referred to primary alcohols.

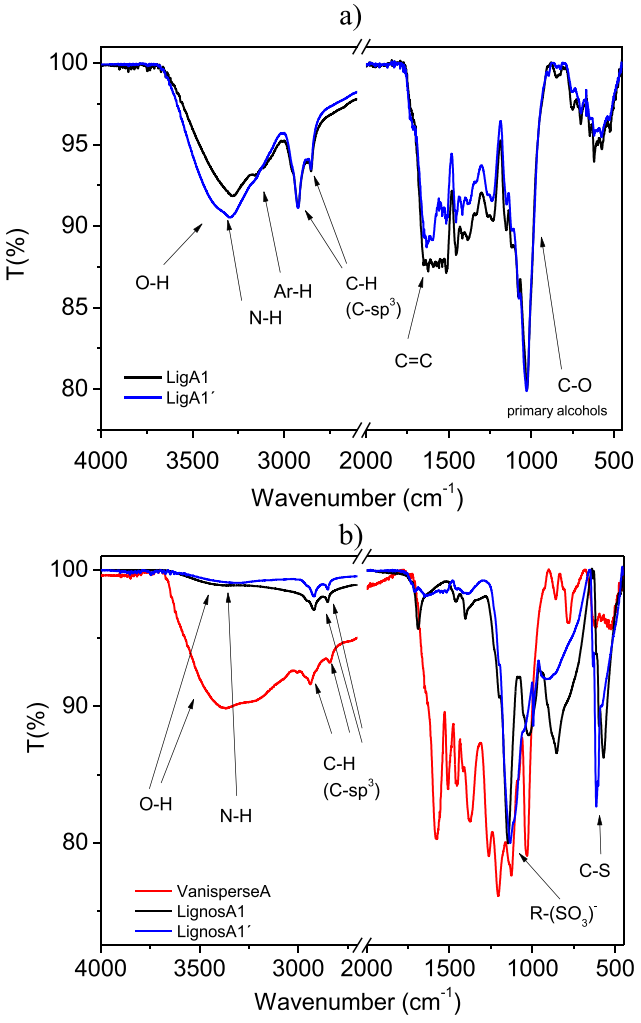

Fig. 2 a) IR spectra of lignins LigA1 and LigA1′; b) IR spectra of lignosulfonates LignosA1, LignosA1′ and Vanisperse A.

The aromatic C-H band appears overlapped by the O-H and / or N-H bands. To confirm the presence of aromatics, a study is carried out using UV–Visible spectroscopy (Fig. A1). To perform this, small amounts of the lignin samples are dissolved in THF. A band observed at 280 nm could be assigned to the presence of aromatic functional groups.

Elemental analysis of lignins and the lignosulfonates obtained after the synthesis show that the percentage of sulfur increases homogeneously, reaching approximately 18%. On the other hand, the percentage of carbon and hydrogen decreases to a great extent, the use of concentrated H_2SO_4 in the synthesis process causes organic matter degradation and dehydration. The %N is provided by the remaining of ionic liquid, used in the extraction process (see Table 1).

As expected, the lignins have almost no sulfur content and, therefore, the degree of sulfonation is practically zero. However, all the lignosulfonates obtained present percentages of sulfur between 12 and 18% and degrees of sulfonation between 4 and 6. These values are much higher than the sulfur content obtained for vanisperse A, which presents a degree of sulfonation of 0.6 (2% of S). In the case of LignosB, used for battery tests, the sulfur content (and degree of sulfonation) is 10 times higher than vanisperse A and indulin AT. Moreover, oak wood presents the lowest sulfur content of all the derivatives studied in this work, which is good agreement with the IR and NMR characterization (see sections 3.2.1 and 3.2.2). The clear conclusion that we obtain from the elemental analysis is that the microwave synthesis of lignosulfonates considerably increases the %S of the starting material. We would like to point out that the expression used to calculate the degree of sulfonation overestimates this parameter because it assumes that all the sulfur content in the sample is in the form of sulfonic acid.

Fig. 2 shows the clear effect in the IR spectrum of the dehydration process. Particularly, we observed a clear loss of the O-H/N-H bands, typical of the sample and from the residual humidity (although we have minimized this option when drying the sample).

Two bands grow clearly in the synthesized lignosulfonates, the first one around 1148–1140 cm^{-1} that refer to organic S = O stretching (R-SO_3H sulfonate group) (Pérez Macías, 2017). In the case of Vanisperse A (commercial lignosulfonate) this signal appears at 1149 cm^{-1} and the second one is assigned to the C-S stretching that appears between 610 and 590 cm^{-1} in the lignosulfonates LignosA1 and LignosA1′. In the case of Vanisperse A, this band appears at 589 cm^{-1} (Ysambertt, 2009).

Based on the results obtained by IR and elemental analysis techniques, it is possible to conclude that the microwave-assisted synthesis was successful for the lignosulfonates production. Moreover, the results of the rest of the lignin samples (see Scheme 2) do not all succeed.

3.2. Comparison between commercial and synthesized lignosulfonates by IR, ^{1}HNMR and COSY

3.2.1. FT-IR-ATR spectroscopic characterization

In the case of commercial (Vanisperse A, Indulin AT, and Oakwood) lignosulfonates, a broad band at approximately

Table 1 Elemental analysis of lignins LigA1 and LigA1′ and all lignosulfonates.

Sample	*Replica*	*%C*	*%H*	*%N*	*%S*	*SD**	*NSD***
LigA1	1°	54.06	6.86	6.52	0.17	0.05	0.08
	2°	54.10	6.73	6.53	0.16		
LigA1′	1°	54.36	6.82	5.15	0.12	0.04	0.07
	2°	53.99	6.68	5.11	0.15		
LignosA1	1°	10.09	3.86	2.09	18.21	5.70	9.11
	2°	9.25	3.52	1.91	18.24		
LignosA1′	1°	9.49	1.62	0.67	18.12	5.70	9.12
	2°	10.71	1.85	0.76	18.36		
LignosA2	1°	0.62	5.44	0.23	16.44	5.14	8.22
	2°	0.65	5.38	0.22	16.43		
LignosA3	1°	2.55	3.85	0.16	17.74	5.31	8.50
	2°	2.58	3.71	0.31	16.24		
LignosB	1°	23.37	5.58	5.19	13.28	4.01	6.41
	2°	24.09	5.77	5.49	12.36		
LignosC1	1°	11.27	2.89	1.04	16.24	4.69	7.50
	2°	10.93	2.80	1.07	13.77		
LignosC2	1°	3.99	3.68	0.38	17.09	5.07	8.11
	2°	4.18	3.53	0.39	15.34		
Vanisperse A	–	–	–	–	2.00	0.63	1
Indulin AT	–	–	–	–	1.64	0.51	0.82
Oak wood	–	–	–	–	less than 0.10	0.03	0.05

*SD means sulfonation degree in mmol of sulfonic acid per gram of lignosulfonate; **NSD means normalized sulfonation degree versus Vanisperse A.

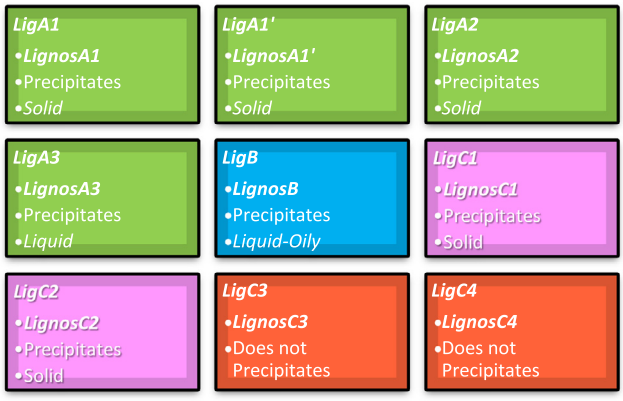

Scheme 2 Overview of Lignosulfonates used in this work. Red boxes indicate failed sulfonation reactions. Green colour: first batch of pruning biomass, all of them give solid precipitate corresponding to lignosulfonate; Blue colour: bagasse biomass, it precipitates at oily lignosulfonate; Violet and red colours: second batch of pruning biomass, violet colour give solid precipitate and red ones does not precipitate. See Schemes A1-A4 and Table A1 of supplementary material for additional information.

3400–3200 cm^{-1} shows the presence of OH groups involved in H-bond networks (Fig. 3). In the synthesized samples, this OH band is also present. We would like to be precise that all the samples have been dried to minimize the humidity content. In the case of the lignosulfonates LignosA2, LignosA3, LignosB, LignosC1, and LignosC2, in principle, the presence of bands due to NH stretching vibrations is also possible as shown in Table 1. Those vibrations are due to the remaining ionic liquid, used in the extraction process. The lignosulfonates LignosA3, LignosC1, and LignosC2 show a narrower vibrational OH band, indicating that they may be owing to less associated alcohols, for example primary, secondary, tertiary alcohols, or phenols.

Regarding the CH region, for commercial lignosulfonates, weak bands around 3000 cm^{-1} are observed indicating the presence of sp^3 C-H stretching. It should be noted that these signals are more intense in the case of Vanisperse A. Both families of lignosulfonates, the synthesized and the commercial ones, also present Ar-H stretching which is overlapped with the OH band (Fig. 3). This fact is in good agreement with the bands observed around 1600–1591 cm^{-1}, which are assigned to C = C stretching, these being aromatic as no clear signal of sp2 carbon C-H tensions appears (Fig. 3).

Lastly, there are the bands that allow establishing a clear connection of the synthesized lignosulfonates with the Vanisperse A, Indulin AT, and Oak wood lignosulfonates and that demonstrate that microwave-assisted sulfonation works successfully. Between 1200 and 1140 cm^{-1}, the bands referring to the S = O stretching of the R- (SO_3) - sulfonates appear. In the case of synthesized lignosulfonates these bands are between 1150 cm^{-1} and 1162 cm^{-1}, in the case of Vanisperse A it appears at 1149 cm^{-1}, in Indulin AT at 1141 cm^{-1} and for Oak wood, it appears at 1158 cm^{-1} (Fig. 3). Likewise, between 1000 and 750 cm^{-1} a band must appear in reference to the S-O tension. This appears, in the case of Vanisperse A, at 851 cm^{-1}, in the case of Indulin AT at 853 cm^{-1}, and for the synthesized lignosulfonates the bands oscillate between 875 cm^{-1} and 850 cm^{-1} (Fig. 3). Around 1030 cm^{-1} stands out a band that is characteristic for all lignosulfonates, both synthesized and commercial and refers to vibrations of S = O of sulfoxide groups (R- (SO) -R). They also appear C-S stretching bands between 710 and 570 cm^{-1}.[15] In the case of Vanisperse A the signal appears at 589 cm^{-1}, for Indulin AT at 624 cm^{-1}, for oak wood at 597 cm^{-1} and for synthesized lig-

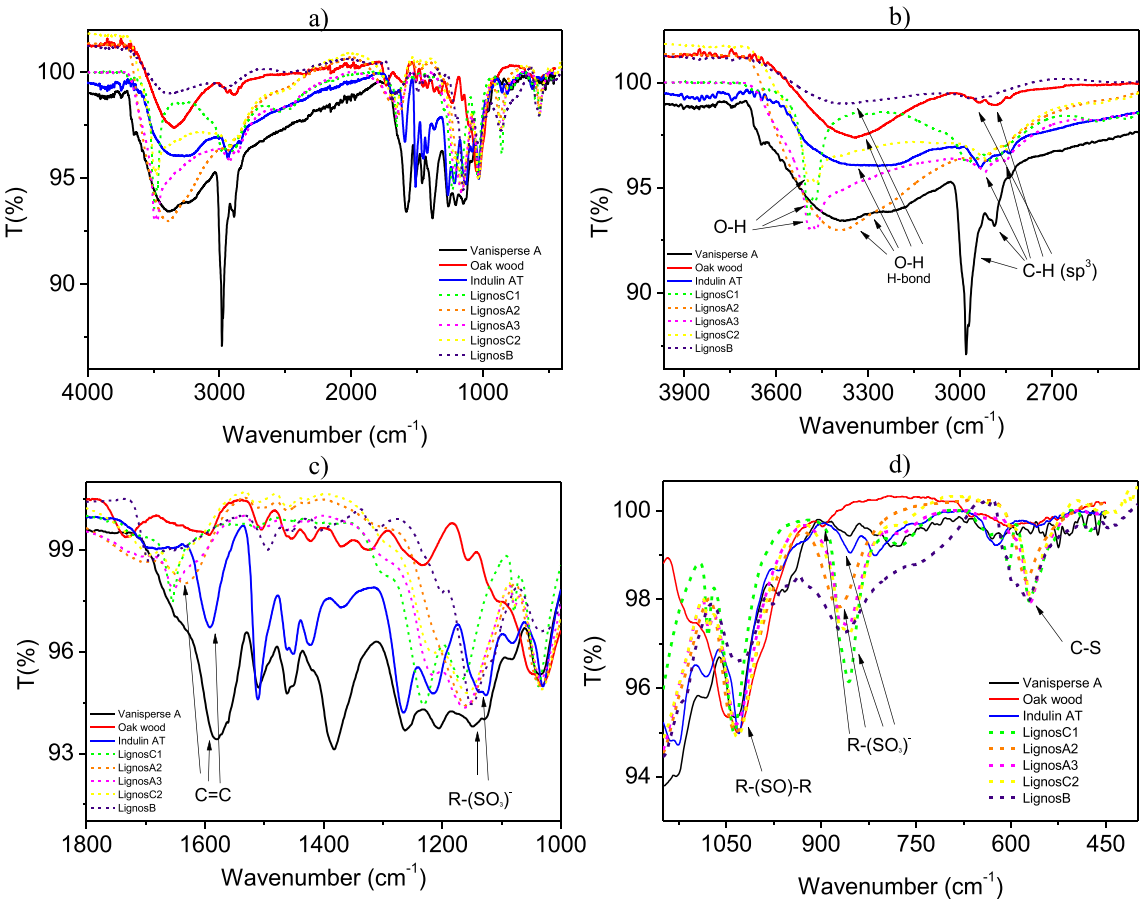

Fig. 3 IR spectra of commercial lignosulfonates and those obtained in this work.

nosulfonates these bands range between 675 cm^{-1} and 570 cm^{-1} (Fig. 3).

3.2.2. ^{1}HNMR and COSY

^{1}HNMR and COSY spectra are very helpful, combined with IR and elemental analysis, to elucidate structural details. Considering the complexity of the structure of lignosulfonates, it was not possible to make a precise assignment for each observed band. Therefore, the assignment of bands is carried out by regions, thus establishing the functional groups that make up the lignosulfonates studied.

In all ^{1}HNMR spectra, the bands that appear at approximately 2.5 ppm, are those corresponding to the solvent used (DMSO), and the bands that appear between 5.25 and 6.5 ppm for lignosulfonates belong to displacements of the H of H_2O (see Figs. 4 and 5). LignosA2 (5.75 ppm), LignosA3 (5.25 ppm), LignosC1 (5.5 ppm), LignosB (6.5 ppm) and LignosC2 (5.5 ppm).

The bands that are observed between 1 ppm and 1.5 ppm correspond to displacements of terminal H of saturated hydrocarbon chains, while the bands located to displacements less than 1 ppm correspond to H in cyclopropanes. Moreover, the displacements between 1.5 and 2.5 ppm are assigned to H displacements of carbons in the alpha position, methylenes, methyls, and alcohols, present in the phenylpropanoid units, establishing that the methyl groups are attached to sulfur or unsaturated carbons. In the case of the lignosulfonates LignosA2 and LignosA3 (Fig. A2), some of the bands that appear may correspond to the remaining solvent used to obtain the lignins, 2-methyltetrahydrofuran, with a signal around 1.73 ppm. The bands between 2.6 ppm and 4 ppm can be assigned to H of methylenes or methyls linked to phenyl, to oxygen, or to H of alcohols. It should be noted that in the case of the lignosulfonate LignosC1 (Fig. A2), the corresponding water band is broad, and signals that are located in the characteristic region of alkenes can overlap (4.5 ppm to 6.5 ppm for terminal H and 4.5 ppm to 8 ppm for H of non-terminal alkenes). Finally, the bands that appear at displacements between 6.5 ppm and 8 ppm can be assigned to displacements of H of aromatic groups, mostly phenyl, taking into account the phenylpropanoid units, phenols, and a less probability to nonterminal alkenes.

In the commercial lignosulfonates, the main difference with the synthesized lignosulfonates is the existence of bands in the range from 4.5 ppm to 6.5 ppm clearly referred to H shifts of alkenes (terminal or not), as in the case of Indulin AT. Besides, there are the aldehyde H displacement bands that appear at approximately 8.6 ppm in the case of Vanisperse A (Fig. 4) and 9.75 ppm in the case of Indulin AT. In the case of oak wood lignosulfonate, these signals are not present.

From the COSY spectra, it can be determined that H are coupled to two or three bonds, being the last one weaker. As can be seen in the spectra represented in Fig. 5, all lignosulfonates, including Vanisperse A, have HH couplings that occur

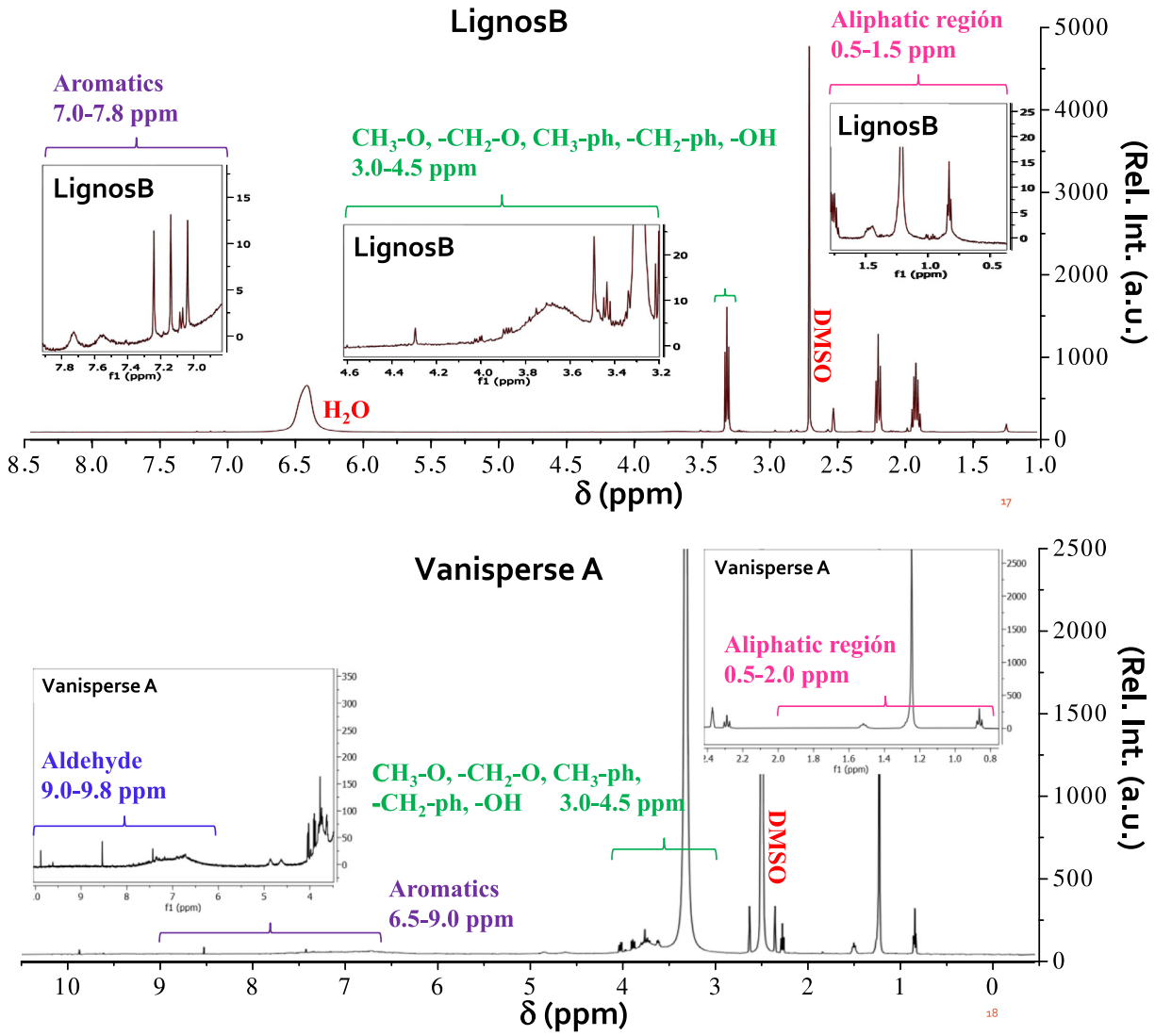

Fig. 4 [1]HNMR spectra of some commercial lignosulfonates and those obtained in this work.

between H of carbon groups in the alpha position, methylenes, methyl groups linked to sulfur or unsaturated carbons, alcohols, and H terminals of saturated hydrocarbon chains. The lignosulfonates LignosB, LignosC2, Indulin AT and Vanisperse A (Fig. 5) also have HH couplings between H of methylene and methyl groups linked to phenyl or oxygen, alcohols, and terminal H chains saturated hydrocarbons. See Fig. A3 for more details about COSY spectra of other commercial a synthetized lignosulfonates not shown in the main text. In the lignosulfonates LignosA3, LignosB, LignosC2 and Indulin AT (Fig. 5), the H couplings of aromatic groups are found (Fig. A3).

The IR comparison spectra of the synthesized lignosulfonates, with respect to the commercial ones, establish that the synthesis is efficient. Furthermore, by analyzing the [1]-HNMR and COSY spectra, it is revealed that the bands obtained are relatively homogeneous, in terms of the groups possessed by the lignosulfonates synthesized in this work.

It should be noted that the LignosA1 and LignosA1 lignosulfonates come from the same pruning biomass sample, and their lignins have undergone the same extraction process. This is a clear indication of the heterogeneity of the material obtained (surely the starting sample is heterogeneous). This effect may be due to slight variations in the percentage of the functional groups that compose them.

In summary, all the lignosulfonates synthesized in this work present some common characteristics, as a high content of S (more than 10%) and the presence of polar aliphatic groups. The content of carbon, hydrogen, and nitrogen are variable, and it seems to be strongly related to the origin of lignin. Moreover, all the lignosulfonates show the presence of aromatic, aliphatic, and polar groups, as Vanisperse A, but in different proportions. However, Vanisperse A presents a high content of aromatic groups in comparison with our lignosulfonates. LignosB present around 25% of C and 13% of S, and IR and NMR reveals the presence of aromatic and polar groups, as in Vanisperse. For that reason, it seems that a reasonable content of C and S is necessary to be used as expander (See section 3.3). Subconsequently, LignosA1 and A1′ present a comparable structure to LignosB but the original lignins

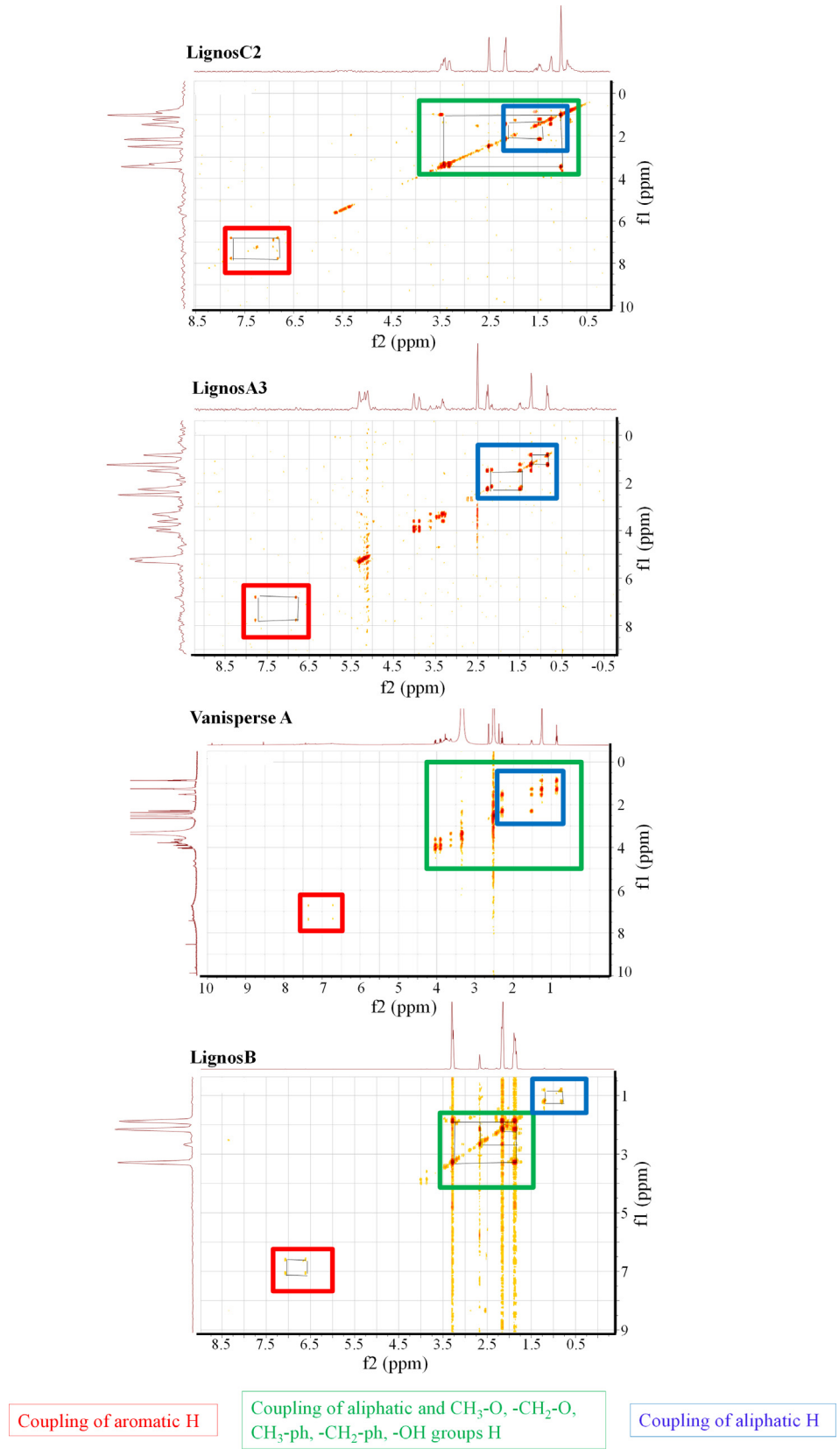

Fig. 5 COSY spectra of commercial lignosulfonates and some of those obtained in this work.

were very heterogeneous and the reproducibility of the sulfonation process was not possible. Finally, LignosA2 and C2 present a low content of C with reveals a different structure in comparison with LignosB and Vanisperse A. However, LignosC2 and A2, together with LignosB showed to be a good choice as expanders.

3.3. Electrochemical characterization

3.3.1. Cyclic voltammetry study

The effects of the addition of commercial and synthesized lignosulfonates on the oxidation/reduction process of the Pb electrode is studied by cyclic voltammetry. These processes are closely related to the charge/discharge processes of the NAM of a Pb/acid battery in the voltage range studied. The obtained i-E polarization curves are shown in Fig. 6. The anodic peak is related to (2) the oxidation of Pb to $PbSO_4$ reaction, while the cathodic peak is represented by the opposite reaction, the reduction of $PbSO_4$ to Pb. Furthermore, the reduction of protons to H_2 (4) occurs in an overlapping way, as a secondary reaction, at more negative potentials.

$$2H^{+}(aq) + 2e^{-} \rightarrow H_2 \quad (4)$$

The charges involved in anodic and cathodic peaks, in the solutions without additives, remain constant in the different tests carried out, although slight variations are observed. In the CV (Fig. 6), sometimes hydrogen formation in the electrochemical cell (-0.8 V to −1 V) occurs irregularly in comparison with the rest of the blank solutions, presumably due to the existence of different roughness of the surface of the Pb electrode which is sanded and cleaned before starting the next measurement since the geometric working area was always the same.

When lignosulfonates are added, changes in both anodic and cathodic processes are observed. This behavior suggests that the addition of 40–60 ppm of lignosulfonate exerts certain modifications, which probably have to do with the adsorption of the lignosulfonates on the Pb surface.

With all the lignosulfonates synthesized, except of LignosA3, the intensity of the redox peaks increases and consequently the Q_{anodic} and $Q_{catodic}$ peaks involved in both processes. This behavior is agreeing with the result obtained with the three commercial lignosulfonates studied (see Fig. 7). This behavior may be due to the adsorption of lignosulfonates affects the structure of the $PbSO_4$ crystal layer obtained. This is reflected in the increase of the accumulated charge in the anodic and the cathodic process, with the lignosulfonate LignosC2 the one that causes the greatest increase. It may happen that, if smaller crystals are obtained, the active area increases, and this may be one of the effects produced. This first study attempts to discriminate between the synthesized materials and verify the effect produced in comparison with commercial lignosulfonates.

In the case of LignosA3, the opposite process occurs, that is, the intensity of the anodic and cathodic peaks is smaller in its presence. The size of the lignosulfonate molecules is a very important factor. In case of large molecules, Pb^{+2} ions could efficiently migrate through the lignosulfonate layers, which form around the working electrode, into the solution. On the opposite, for small size molecules, the accumulation of Pb^{+2} ions between the layers leads to an accumulation of Pb^{+2} ions, which hinders the redox reactions (Pérez Macías, 2017).

The increase in Q_{red} keeps the same relationship as Q_{ox} and may be related to charge acceptance when the material is conformed as a negative element of the battery, this previous study in a three-electrode cell may be an interesting test to discriminate between previously obtained materials for the subsequent battery test.

Finally, LignosB was selected as a good candidate as an expander for battery tests for many reasons: first, the presence of aromatics and polar groups is comparable to that of Vanisperse A; second, the homogeneity of the original lignins and the corresponding sulfonation process make it reproducible; third, the charge tests from i-E curves showed a good performance; fourth, it seems that the percentage of C and S should be enough for a good performance; and fifth, the N content is not yet clear because high content of N if the content of C and H is also high, seems to be important. However, lignosulfonates with low C, H and N content also show good performance in charge tests.

3.3.2. Study in Pb/acid battery of 0,23Ah.

During the formation procedure, the first charging step (0.0736 A) was quickly reached by the cells, easily getting the capacity limit (0.096 Ah). In the second charging step, a better forma-

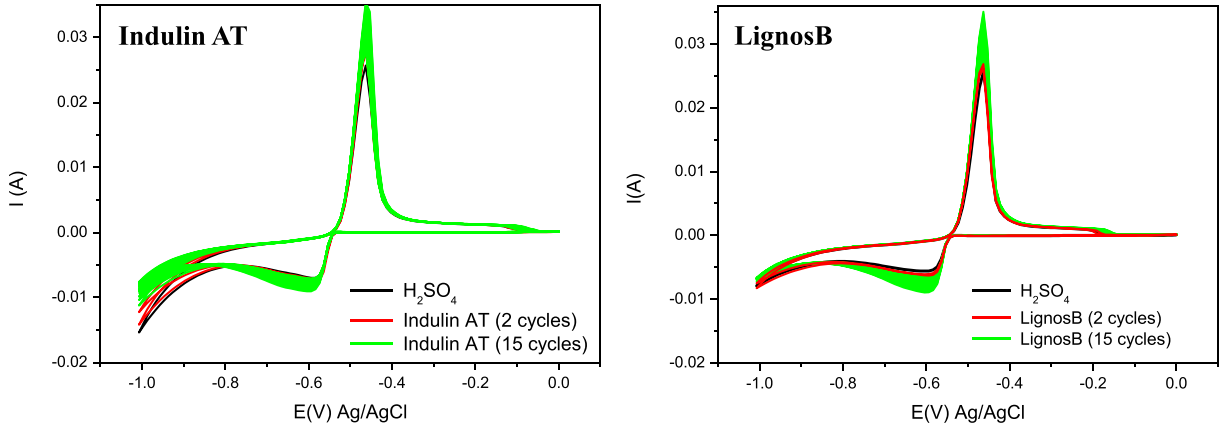

Fig. 6 CV at 5 mV/s and room temperature (25 °C) of commercial lignosulfonate Indulin AT and that obtained in this work LignosB. The working electrode (Pb) used has an $A_{geometric}$ of 1,16 cm^2.

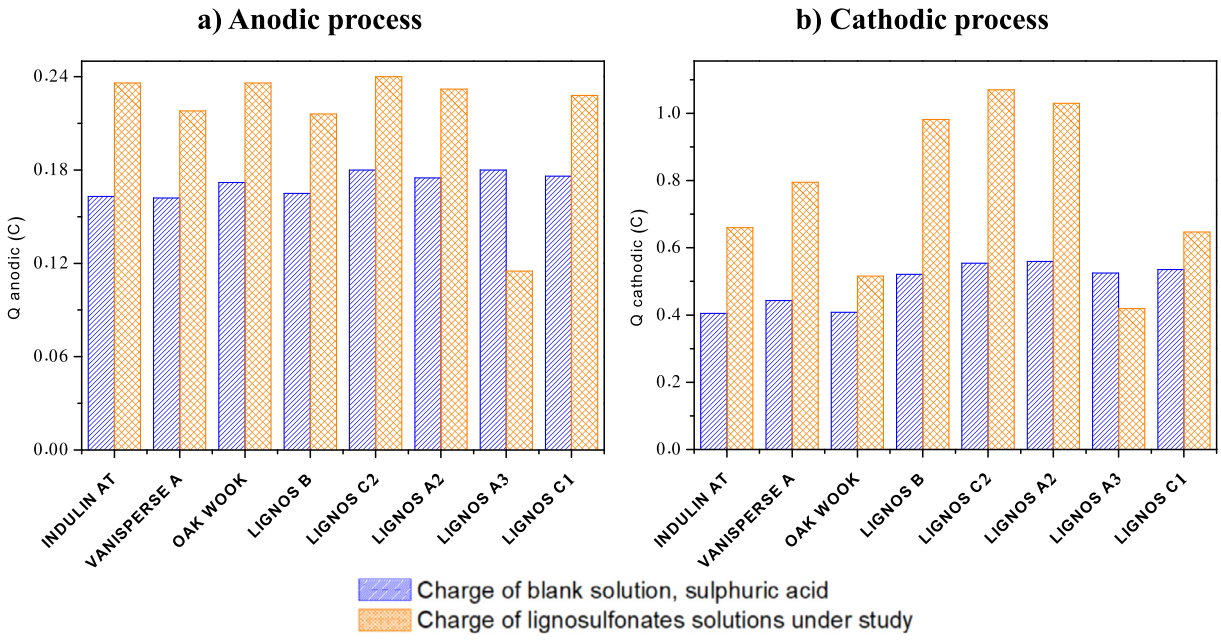

Fig. 7 Charge from i-E curves anodic (a) and cathodic (b) processes. Blank (blue), Lignosulfonate (Orange).

tion was shown by LignosB Cells, since the capacity limit of 0.166 Ah was reached with a lower voltage value (around 2.40 V), instead to around 2.85 V reached by the Contol Lig Cells (with Vanisperse A) in the same step. A similar trend in the third charging step (0.0368 A) was found. Thus, a better formation was revealed by LignosB Cells, showing lower electric resistance and smoother charging steps. After cell formation, the initial voltage and internal resistance were measured, obtaining average values of 2.18 V and 68 mOhm.

After the battery formation, some electrical tests were performed, consisting of two C_{20} Capacity tests, a Charge Acceptance (CA) test, and a pseudo-Tafel test, see Figs. 8 and 9.

C_{20} *Capacity test*: In the 1st capacity, the results of Control Lig Cells were improved by LignosB Cells, with an increment of 36.30%. However, in the 2nd capacity, similar values were obtained. According to the better formation by LignosB Cells, the 1st capacity was improved. But, in the 2nd capacity where the effects from the previous formation are almost non-existent, all cells a showed a similar capacity.

Charge Acceptance test (CA test): LignosB Cells showed superior results, reaching an improvement of 63.16%. Thus, the reversibility of the negative plate was improved by the new sugar cane lignosulfonate compared to the Control Lig Cells, it is important to remember that this cell includes Vanisperse A.

Pseudo-Tafel test: The Tafel slopes of the test were observed to be a little far from the theoretical one (-0.120 V/dec). Therefore, the results could be slightly affected by other secondary mechanisms during the measurement. The values were −0.195 and −168 V/dec for Control Lig Cells and LignosB Cells respectively. Furthermore, the Hydrogen Evolution Reaction (HER) was slightly increased with the new lignosulfonate LignosB compared to Vanisperse A. Since the η_0 (HER) with LignosB Cell presents a positive overpotential

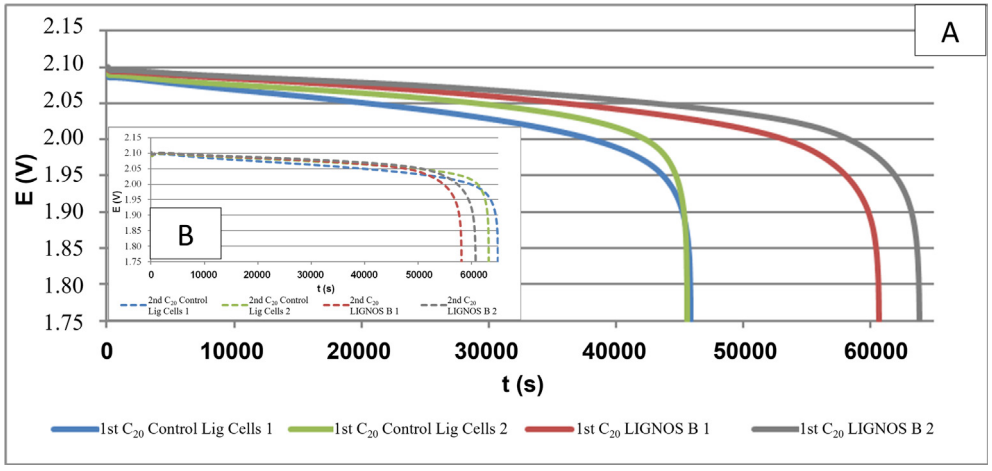

Fig. 8 First (A) and second (B) capacity tests. Comparison of control cells withs those containing Lignos B.

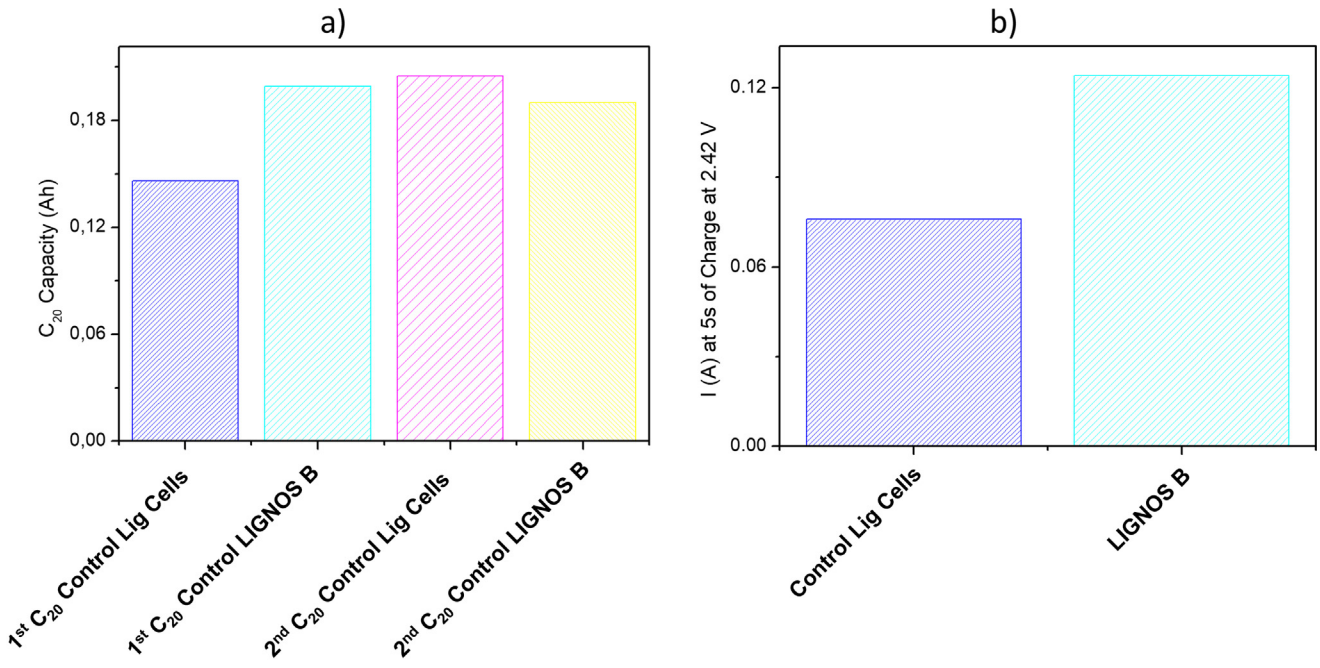

Fig. 9 Pb/acid battery tests: a) First and second capacity; b) Charge Acceptance test.

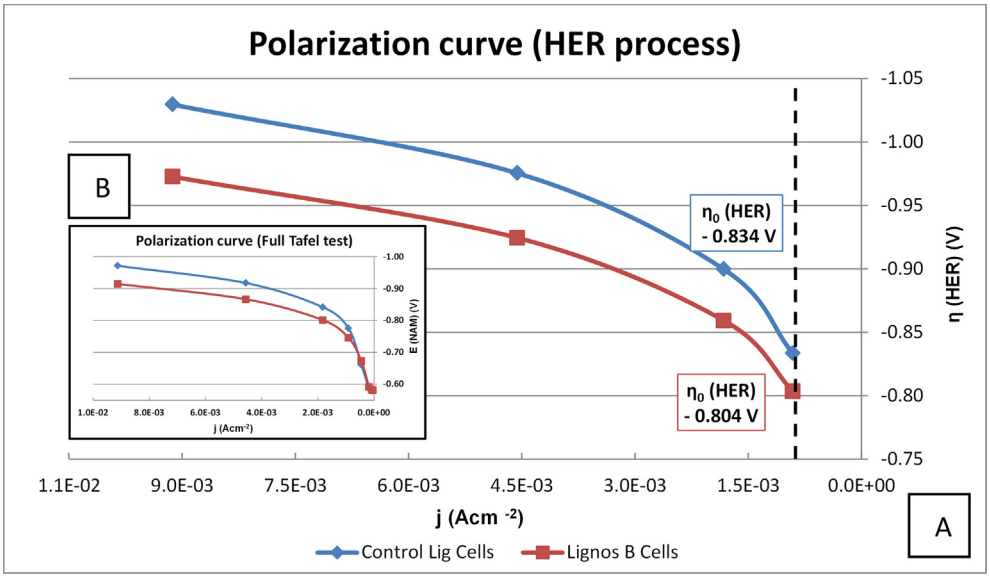

Fig. 10 Pb/acid control battery Cathode polarization. Detail on HER process (A) and full Tafel test (B).

around 30 mV (see Fig. 10) vs the Control Lig Cells, the HER production will be easier with the new LignosB studied in the new cell.

It is shown that the incorporation of LignosB improves the cell formation as well as the first capacity and the charge acceptance, these parameters being relevant in the performance of Pb/acid batteries. Nevertheless, the effect of LignosB vs Vanisperse A on the ease of HER generation is not a positive result as it does not improve the performance of the Pb/acid battery. This study intended to be the beginning of a more in-depth work that has allowed the use of lignins obtained from pruning and sugarcane biomass that has been transformed to lignosulfonates with a simple process and that have been subsequently tested as expanders.

In future work, the implementation of higher capacity batteries of 1Ah and then 60Ah batteries will be carried out. Furthermore, the addition of Carbon to the negative element of the battery will be considered to obtain better results. Nonetheless, as indicated above, the formula analyzed does not correspond exactly to the usual Pb/acid battery mixture.

4. Conclusions

Once the study presented has been carried out, it can be concluded that:

Lignin's from pruning and cane biomass have been characterized and derivatized as lignosulfonates.

The synthesis process is not efficient for all lignin samples, as is the case with the LigC3 and LigC4. Although these come from the same pruning biomass, the extraction method is different, causing variations in the unions and proportions of the phenylpropanoid units.

The characterization of the lignosulfonates establishes, on the one hand, that the chosen synthesis method (by microwave-assisted) was successful and, that they have the same functional groups (but in variable proportion).

According to the cycle voltammetry study, the lignosulfonates synthesized fulfill their function (except for the lignosulfonate LignosA3), since they maintain a similar behavior to the commercial lignosulfonates: Vanisperse A, Indulin AT and Oak Wood.

Their adsorption on the working electrode causes an increase in the charge, both in the anodic and cathodic process, indicating their effectiveness in controlling the formation of $PbSO_4$ crystals. In the case of the lignosulfonate LignosA3 does not follow a similar pattern; this may be linked to the size of the molecules that compose it, as well as to the presence of different functional groups from the rest of the synthesized lignosulfonates.

Regarding the study of Pb/acid battery, the functionality of LignosB as an expander improves the cell formation as well as the first capacity (C_{20}) and the charge acceptance compared to Vanisperse A, these parameters being very important for the performance of the Pb/acid battery. However, a positive hydrogen evolution overpotential around 30 mV is obtained from LignosB compared to Vanisperse A. However, we consider that it constitutes a first approach to future work with higher capacity batteries.

Declaration of Competing Interest

The authors declare that they have no known competing financial interests or personal relationships that could have appeared to influence the work reported in this paper.

Acknowledgements

This work was supported by the Comunidad de Madrid (Spain) and ERDF (European Regional Development Fund), grant number S2018/EMT-4344 (BIOTRES-CM) and Grant PID2020-112594RB-C33 funded by MCIN/AEI/10.13039/501100011033.

Appendix A. Supplementary material

Supplementary data to this article can be found online at https://doi.org/10.1016/j.arabjc.2022.104127.

References

Awosusi, A.A., Ayeni, A., Adeleke, R., Daramola, M.O., 2017. Effect of water of crystallization on the dissolution efficiency of molten zinc chloride hydrate salts during the pre-treatment of corncob biomass. J. Chem. Technol. Biotechnol. 92, 2468–2476. https://doi.org/10.1002/jctb.5266.

Aro, T., Pedram, F., 2017. Production and application of lignosulfonates and sulfonated lignin. ChemSusChem. 10, 1861–1877. https://doi.org/10.1002/cssc.201700082.

Baumberger, S., Lapierre, C., Monties, B., Lourdin, D., Colonna, P., 1997. Preparation and properties of thermally moulded and cast lignosulfonates-starch blends. Indus. Crops Prod. 6 (6), 253–258. https://doi.org/10.1016/S0926-6690(97)00015-0.

Behera, S., Arora, R., Nandhagopal, N., Kumar, S., 2014. Importance of chemical pretreatment for bioconversion of lignocellulosic biomass. Renew. Sustain. Energy Rev. 36, 91–106. https://doi.org/10.1016/j.rser.2014.04.047.

M. Chávez Sifontes, M. E. Domine, Lignin, structure and applications: depolymerization methods for obtaining aromatic derivatives of industrial interest, Av. cien. ing. 4(4) (2013) 15-46. ISSN-e 0718-8706.

Crestini, C., Melone, F., Sette, M., Saladino, R., 2011. Milled wood lignin: a linear oligomer. Biomacromolecules 12, 3928–3935. https://doi.org/10.1021/bm200948r.

Dutta, T., Papa, G., Wang, E., Sun, J., Isern, N.G., Cort, J.R., Simmons, B.A., Singh, S., 2018. Characterization of lignin streams during bionic liquid-based pretreatment from grass, hardwood, and softwood. ACS Sustain. Chem. Eng. 6 (6), 3079–3090. https://doi.org/10.1021/acssuschemeng.7b02991.

Grande, P.M., Viell, J., Theyssen, N., Marquardt, W., Domínguez de María, P., Leitner, W., 2015. Fractionation of lignocellulosic biomass using the OrganoCat process. Green Chem. 17, 3533–3539. https://doi.org/10.1039/C4GC02534B.

Gu, L., Jiang, B., Song, J., Jin, Y., Xiao, H., 2019. Effect of lignin on performance of lignocellulose nanofibrils for durable superhydrophobic surface. Cellulose 26, 933–944. https://doi.org/10.1007/s10570-018-2129-0.

Guo, S., Li, X., Kuang, Y., Liao, J., Liu, K., Li, J., Mo, L., He, S., Zhu, W., Song, J., Song, T., Rojas, O.J., 2021. Residual lignin in cellulose nanofibrils enhances the interfacial stabilization of Pickering emulsions. Carbohydr. Polym. 253,. https://doi.org/10.1016/j.carbpol.2020.117223 117223.

Lara-Serrano, M., Morales-delaRosa, S., Campos-Martín, J.M., Fierro, J.L.G., 2019. Fractionation of lignocellulosic biomass by selective precipitation from ionic liquid dissolution. Appl. Sci. 9 (9), 1862. https://doi.org/10.3390/app9091862.

Lara-Serrano, M., Morales-delaRosa, S., Campos-Martín, J.M., Fierro, J.L.G., 2020. High enhancement of the hydrolysis rate of cellulose after pretreatment with inorganic salt hydrates. Green Chem. 22, 3860–3866. https://doi.org/10.1039/D0GC01066A.

Lavarda, G., Morales-delaRosa, S., Centomo, P., Campos-Martin, J. M., Zecca, M., Fierro, J.L.G., 2019. Gel-type and macroporous cross-linked copolymers functionalized with acid groups for the hydrolysis of wheat straw pretreated with an ionic liquid. Catalysts 9 (8), 675. https://doi.org/10.3390/catal9080675.

Li, Q., Zeng, M., Zhu, D., Lou, H., Pang, Y., Qiu, K., Huang, J., Qiu, X., 2019. A simple and rapid method to determine sulfonation degree of lignosulfonates. BioEnergy Res. 12, 260–266. https://doi.org/10.1007/s12155-019-09972-x.

Liu, T., Wang, P., Tian, J., Guo, J., Zhu, W., Jin, Y., Xiao, H., Song, J., 2022. Polystyrene sulfonate is effective for enhancing biomass enzymatic saccharification under green liquor pretreatment in bioenergy poplar. Biotechnol. Biofuels Bioprod. 15, 10. https://doi.org/10.1186/s13068-022-02108-y.

Lou, H., Zhou, H., Li, X., Wang, M., Zhu, J.Y., Qiu, X., 2014. Understanding the effects of lignosulfonate on enzymatic saccharification of pure cellulose. Cellulose 21, 1351–1359. https://doi.org/10.1007/s10570-014-0237-z.

Myrvold, B.O., 2003. Interactions between lignosulphonates and the components of the lead-acid battery: part 1. adsorption isotherms. J. Power Sources 117, 187–202. https://doi.org/10.1016/S0378-7753(03)00018-1.

Pavlov, D., 1984. Power Sources for Electric Vehicles. Elsevier, Amsterdam.

D. Pavlov, P. Nikolov, T. Rogachev, Influence of expander components on the processes at the negative plates of lead-acid cells on high-rate partial-state-of-charge cycling. Part I: Effect of lignosulfonates and $BaSO_4$ on the processes of charge and discharge of negative plates, J. Power Sources 195 (2010) 4435–4443. https://doi.org/10.1016/j.jpowsour.2009.11.060; W:R. Kitchens, R.C. Osten, D.W.H. Lambert, Advances in manufacturing systems for the production of pastes for lead/acid battery plates, J. Power Sources 53 (1995) 263-267. https://doi.org/10.1016/0378-7753(94)02020-4; D.P. Boden, Selection of pre-blended expanders for optimum lead/acid battery performance, J. Power Sources 73 (1998) 89–92. https://doi.org/10.1016/S0378-7753(98)00026-3.

Pavlov, D., Myrvold, B.O., Rogachev, T., Matrakova, M., 2000. A new generation of highly efficient expander products and correlation between their chemical composition and the performance of the lead–acid battery. J. Power Sources 85, 79–91. https://doi.org/10.1016/S0378-7753(99)00386-9.

Pérez Macías, M.A., 2017. Análisis del tipo de lignina en mezclas de lignina/carbón en expansores para la optimización de baterías de plomo-ácido. Universidad Autónoma de Nuevo León, Mexico. PhD Thesis.

Pickett, J., 2018. Sustainable Biofuels: Prospects and Challenge. The Royal Society, London, UK.

D. A. J. Rand, J. Garche, P:T. Moseley, C.D. Parker, Valve-Regulated Lead-Acid Batteries. Editorial Elsevier Science, 2004. ISBN: 9780080474731.

Reyes, H., Rodríguez, J., Cardona, L., 2015. Lignin electrotransformation analysis in bamboo "Angustifolia Kunth" from the colombian Quindío department. Rev. Cienc. en Desarro. 6, 55–60. https://doi.org/10.19053/01217488.3649.

Rubin, E.M., 2008. Genomics of cellulosic biofuels. Nature 454, 841–845. https://doi.org/10.1038/nature07190.

Ruetschi, P., 1977. Review on the lead—acid battery science and technology. J. Power Sources 2, 3–120. https://doi.org/10.1016/0378-7753(77)85003-9.

Stiefel, S., Di Marino, D., Eggert, A., Kühnrich, I.R., Schmidt, M., Grande, P.M., Leitner, W., Jupkec, A., Wessling, M., 2017. Liquid/liquid extraction of biomass-derived lignin from lignocellulosic pretreatments. Green Chem. 19, 93–97. https://doi.org/10.1039/C6GC02270G.

Tang, Q., Qian, Y., Yang, D., Qiu, X., Qin, Y., Zhou, M., 2020. Lignin-based nanoparticles: a review on their preparations and applications. Polymers 12, 2471. https://doi.org/10.3390/polym12112471.

Tian, J., Yang, Y., Song, J., 2019. Grafting polycaprolactone onto alkaline lignin for improved compatibility and processability. Int. J. Biol. Macromol. 14, 919–926. https://doi.org/10.1016/j.ijbiomac.2019.09.055.

Vermaas, J.V., Petridis, L., Qi, X., Schulz, R., Lindner, B., Smith, J.C., 2015. Mechanism of lignin inhibition of enzymatic biomass deconstruction. Biotechnol. Biofuels 8, 217. https://doi.org/10.1186/s13068-015-0379-8.

Wang, P., Liu, T., Liu, Y., Tian, J., Zhang, X., Guo, J., Jin, Y., Xiao, H., Song, J., 2021. In-situ and real-time probing cellulase biosensor formation and its interaction with lignosulfonate in varied media. Sensor Actuat. B Chem. 329,. https://doi.org/10.1016/j.snb.2020.129114 129114.

Wang, P., Wang, Q., Liu, T., Guo, J., Jin, Y., Xiao, H., Song, J., 2022. Exploring the promoting mechanisms of bovine serum albumin, lignosulfonate, and polyethylene glycol for lignocellulose saccharification from perspective of molecular interactions with cellulase. Arabian J. Chem. 15,. https://doi.org/10.1016/j.arabjc.2022.103910 103910.

Weidener, D., Leitner, W., Domínguez de María, P., Klose, H., Grande, P.M., 2021. Lignocellulose fractionation using recyclable phosphoric acid: lignin, cellulose, and furfural production. ChemSusChem. 14, 909–916. https://doi.org/10.1002/cssc.202002383.

Yang, H., Qiu, Y., Guo, Y.X., 2017. Lead oxide/carbon black composites prepared with a new pyrolysis-pickling method and their effects on the high-rate partial-state-of-charge performance of lead-acid batteries. Electrochim. Acta 235 (235), 409–421. https://doi.org/10.1016/j.electacta.2017.03.138.

Yao, M., Yang, Y., Song, J., Yu, Y., Jin, Y., 2017. Lignin-based catalysts for Chinese fir furfurylation to improve dimensional stability and mechanical properties. Ind. Crop. Prod. 107, 38–44. https://doi.org/10.1016/j.indcrop.2017.05.038.

F. Ysambertt, Propiedades tensoactivas de la lignina extraída del "licor negro" modificada por reacciones asistidas por microondas, Rev. Cuba. Química 21 (2009) 65–75. ISSN: 0258-5995. https://www.redalyc.org/articulo.oa?id=443543718008.

Zhang, Y., Mei, H., Cao, Y., Yan, X., Yan, J., Gao, H., Luo, H., Wang, S., Jia, X., Kachalova, L., Yang, J., Xue, S., Zhou, C., Wang, L., Gui, Y., 2021. Recent advances and challenges of electrode materials for flexible supercapacitors. Coord. Chem. Rev. 438,. https://doi.org/10.1016/j.ccr.2021.213910 213910.

Zhang, Y., Zhou, C., Yang, J., Xue, S., Gao, H., Yan, X., Huo, Q., Wang, S., Cao, Y., Yan, J., Gao, K., Wang, L., 2022. Advances and challenges in improvement of the electrochemical performance for lead-acid batteries: a comprehensive review. J. Power Sources 520,. https://doi.org/10.1016/j.jpowsour.2021.230800 230800.